Supplementary Figure S1

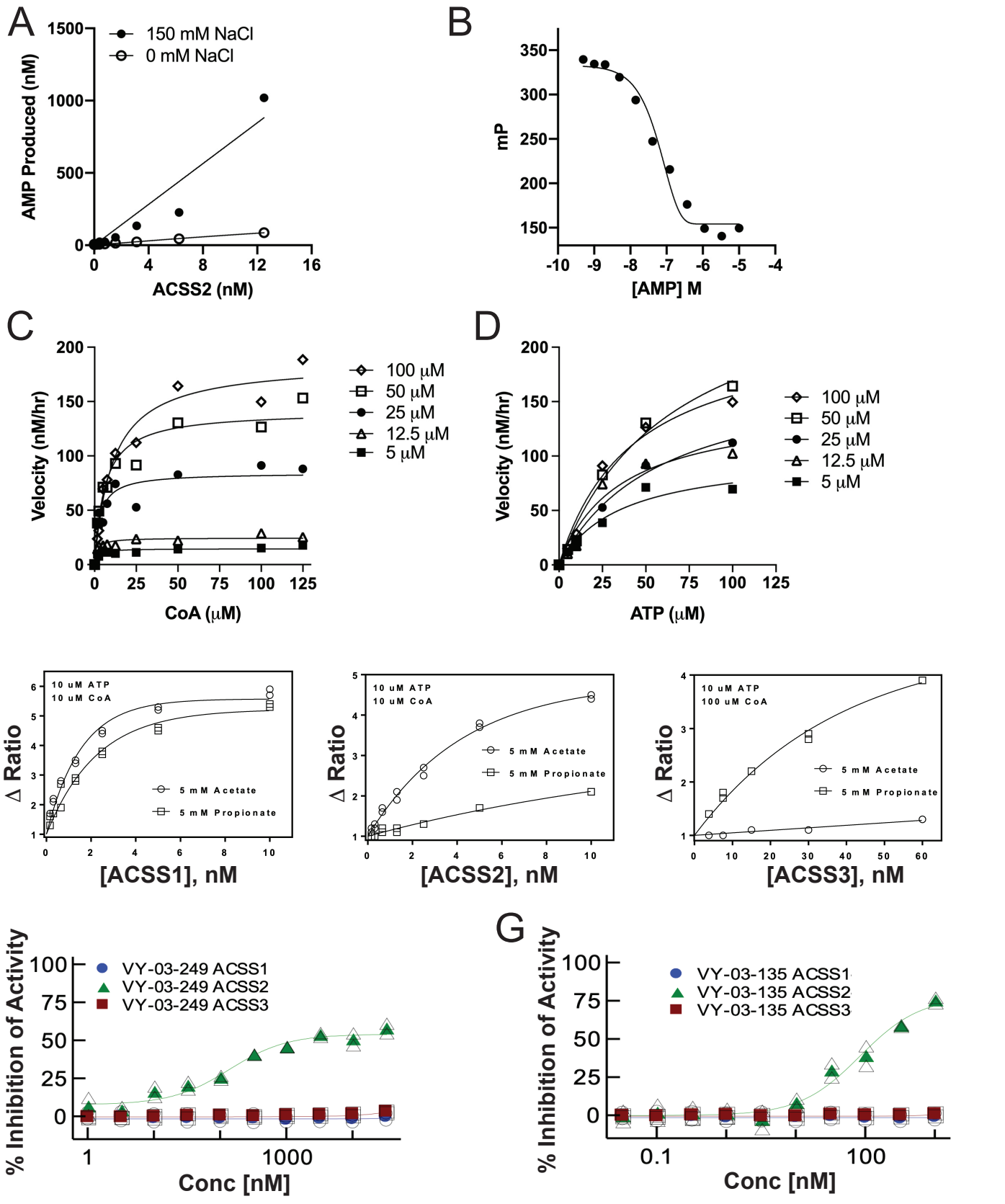

Supplementary Figure S1. VY-3-135 does not affect ACSS1 or ACSS3 activity in vitro. (A) Enzyme titration in the presence and absence of 150mM NaCl using a 2-fold serial dilution starting at 100 nM. n = 1. (B) AMP standard curve using a 3-fold serial dilution starting at 10 μM. (C-D) Km and Vmax determination for coenzyme A and ATP. Concentrations of reactants ranged from 5 μM to 100 μM. n = 1. (E) Specificity of ACSS1, ACSS2 and ACSS3 for acetate and propionate at increasing concentrations of enzyme. (F-G) Dose response curves shown as percent inhibition of activity for VY-3-249 (*panel F*) and VY-3-135 (*panel G*) for ACSS1, ACSS2 and ACSS3 with propionate as the substrate.

Supplementary Figure S2

A

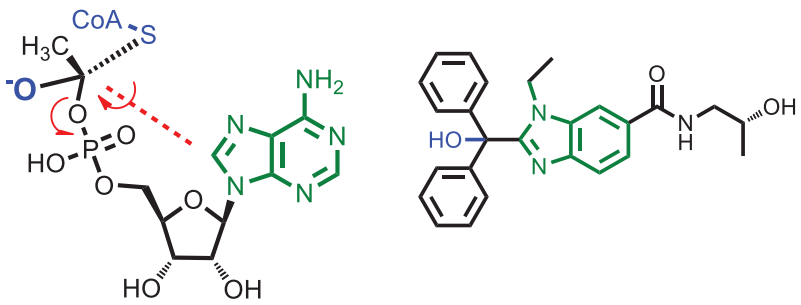

B

Cluster	Cluster Rank	ΔG
Site 1 (Acetyl-AMP)		
0	0	-9.453925
0	1	-9.227344
0	2	-8.449596
0	3	-8.503612
0	4	-7.43013
Site 2		
1	0	-8.465773
1	1	-8.414994
1	2	-8.401743
1	3	-8.401743
1	4	-8.162664
1	5	-8.162664
1	6	-8.162664
1	7	-8.192092
1	8	-8.192092
1	9	-8.048429
1	10	-8.048429
1	11	-8.048429
1	12	-7.0162835
1	13	-7.0162835
1	14	-7.4958844
1	15	-6.8667297

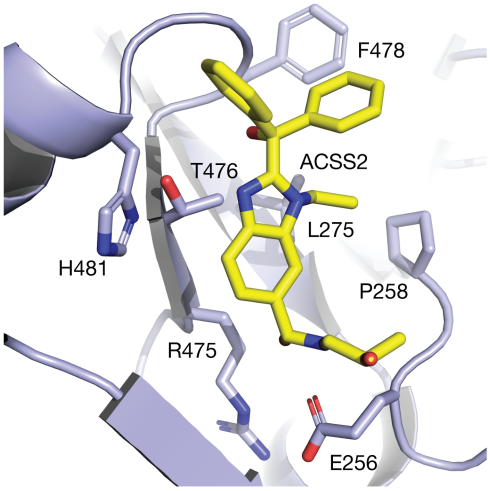

Supplementary Figure S2. VY-3-135 is predicted to be a transition state mimetic of ACSS2. (A) The adenine moiety (green) is in close proximity to the oxyanion (blue) in the reaction center which suggests that the alcohol moiety (blue) in VY-3-135 (*panel B*) is mimicking the oxyanion and the benzimidiazole is mimicking the adenine. (B) ΔG data of VY-3-135 binding to site 1 and 2 of acetyl-CoA synthetase generated by SwissDock. Second acetyl-CoA synthetase binding site of VY-3-135.

Supplementary Figure S3

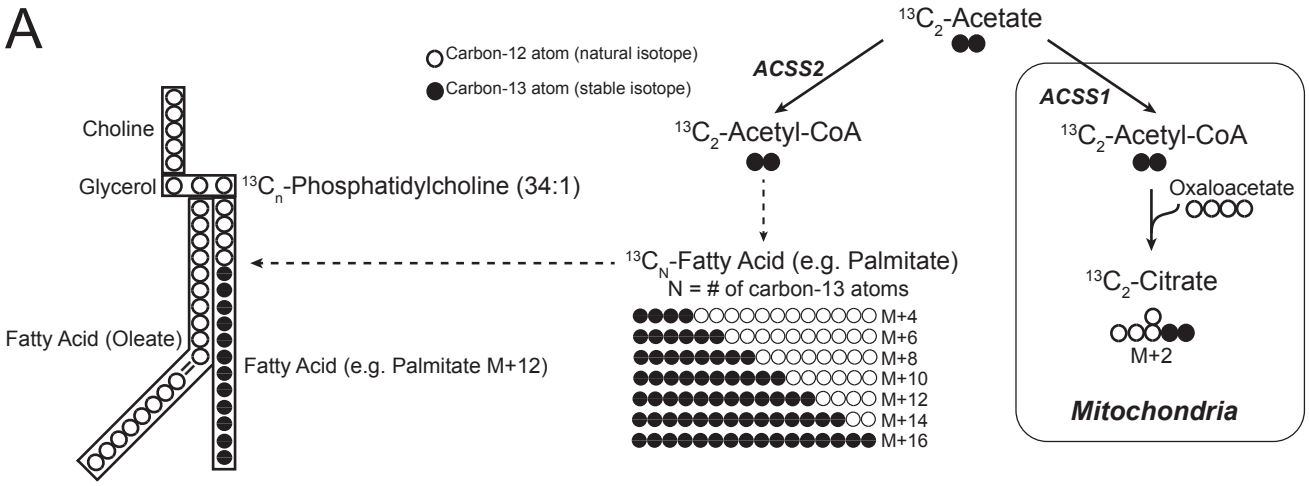

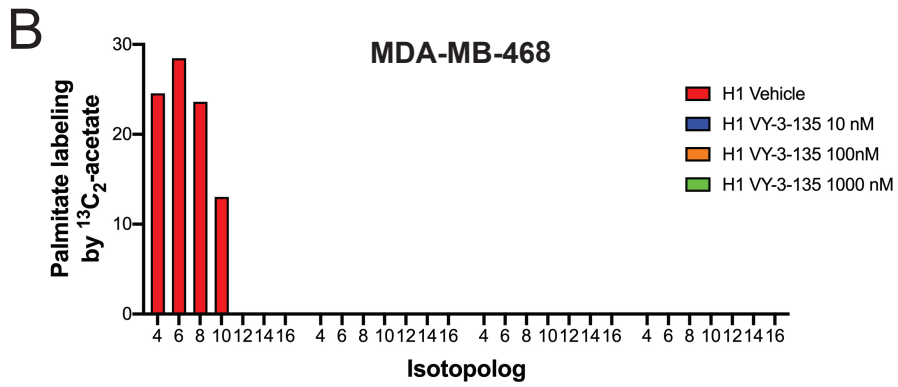

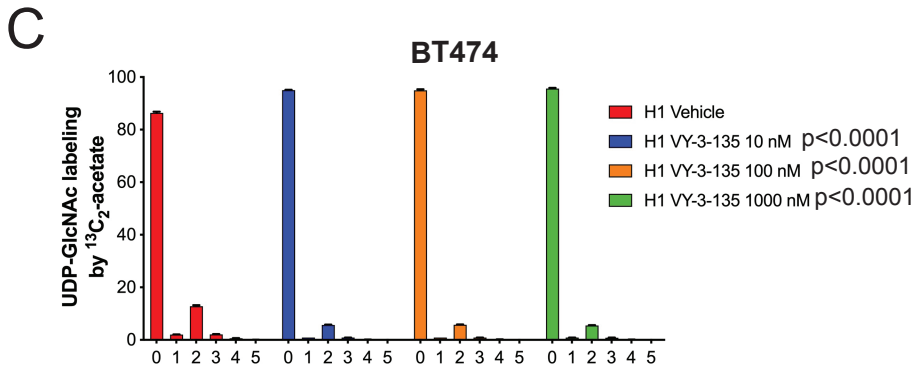

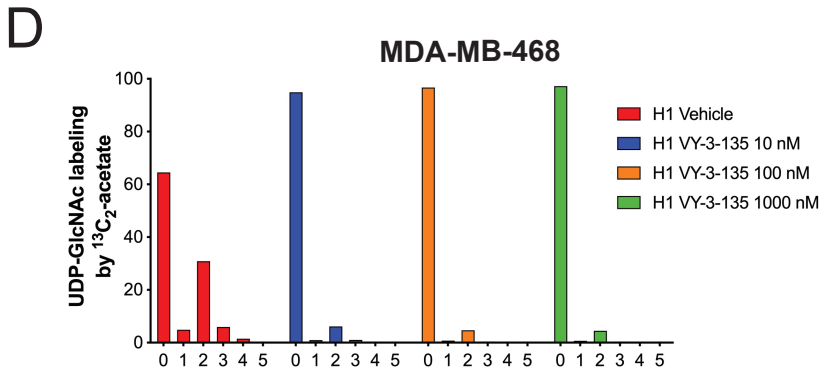

Supplementary Figure S3. VY-3-135 is a potent inhibitor of ACSS2 in cells. (A) Schematic of stable isotope tracing of $^{13}C_2$-acetate into citrate, fatty acids, and phospholipids. (B) Enrichment of 100 μM $^{13}C_2$-acetate into palmitate in MDA-MB-468 cells cultured in H1 conditions over a 24hr period using a 10-fold serial dilution of VY-3-135. n = 1. (C-D) Enrichment of $^{13}C_2$-acetate into the UDP-GlcNAc pool of BT474 cells (*panel C*) (n=3) and MDA-MB-468 cells (*panel D*) (n=1). Experimental parameters were identical to panel B.

Supplementary Figure S4

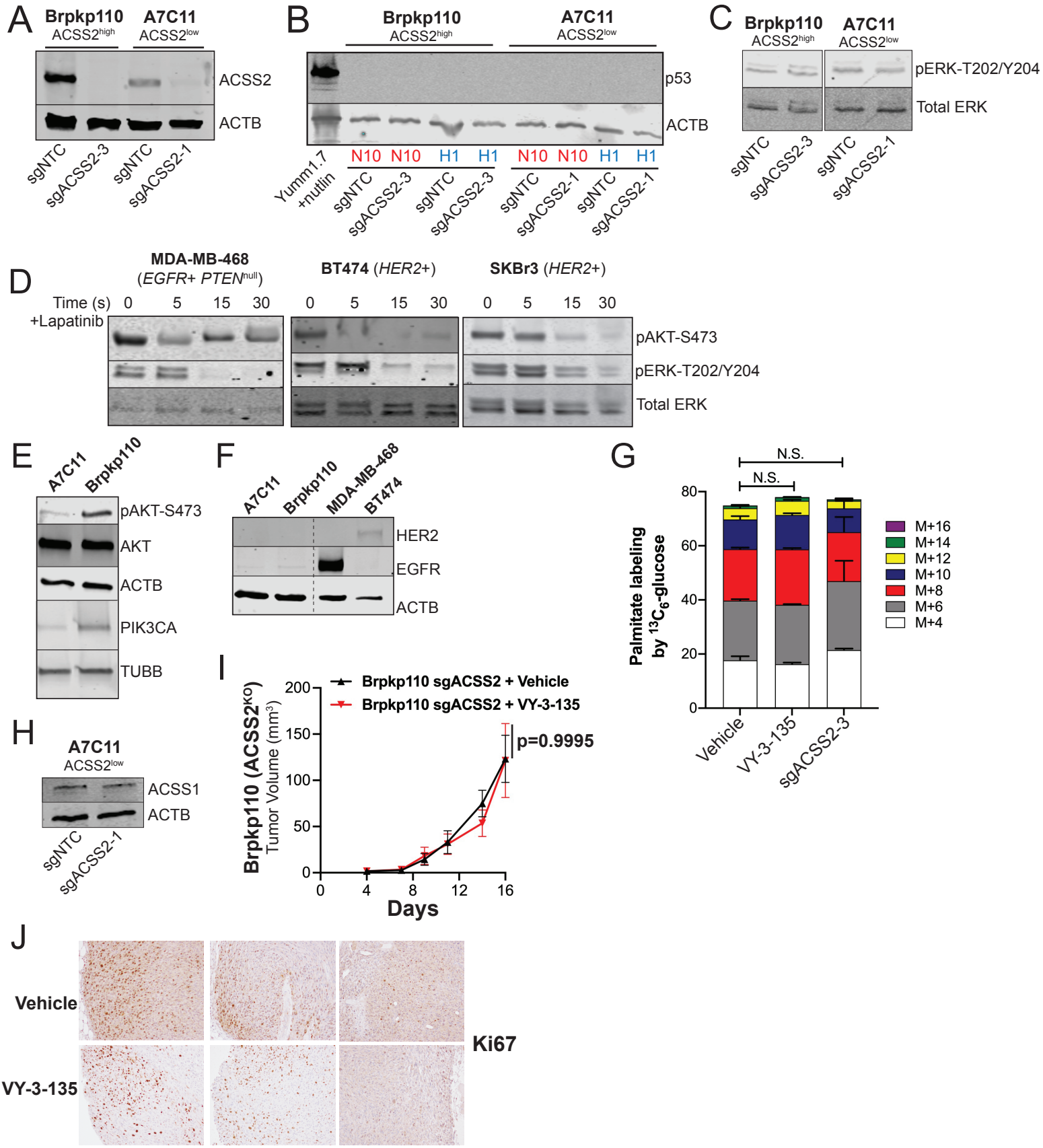

Supplementary Figure S4 VY-3-135 does not affect the growth of ACSS2 knockout tumors. (A) Immunoblot for ACSS2 in A7C11 and Brpkp110 *Acss2* CRIPSR knockout cell lines. (B) Immunoblot for TP53 in A7C11 and Brpkp110 *Acss2* CRIPSR knockout cell lines in N10 and H1 culture conditions. Lysates from Yumm1.7 (p53 positive) melanoma cell treated with nutlin to stabilize p53 are the positive control. (C) Immunoblot for phosphorylated ERK (p42/p44 T202/Y204) as a readout of MAP kinase pathway activation in A7C11 and Brpkp110 cell lines. (D) MDA-MB-468, BT474 and SKBr3 human breast cancer cells were treated with 500 nM lapatinib for the indicated times. Cell lysates were immunobloted for phosphorylated AKT and phosphorylated ERK. Total ERK is the loading control. (E) Immunoblot for phosphorylated AKT and total PI3K in A7C11 and Brpkp110 breast cancer cells. (F) Immunoblot for HER2 and EGFR in A7C11, Brpkp110, MDA-MB-468 and BT474 cell lines. All bands are from the same gel and exposure. (G) Fractional abundance (% labeling) of palmitate by $^{13}C_6$-glucose in Brpkp110 cells in N10 culture conditions in the presence and absence of 1 μM VY-3-135. (H) Immunoblot for ACSS1 in A7C11 sgNTC and sgACSS2 cells. (I) VY-3-135 treatment did not further affect the growth of Brpkp110 sgACSS2 tumors that lack expression of ACSS2. Data represent mean ± S.E.M. with ANOVA p value displayed, n = 5. B). (J) Ki67 immunohistochemistry staining of vehicle and VY-3-135 treated tumors. n = 3 per treatment group.

Supplementary Figure S5

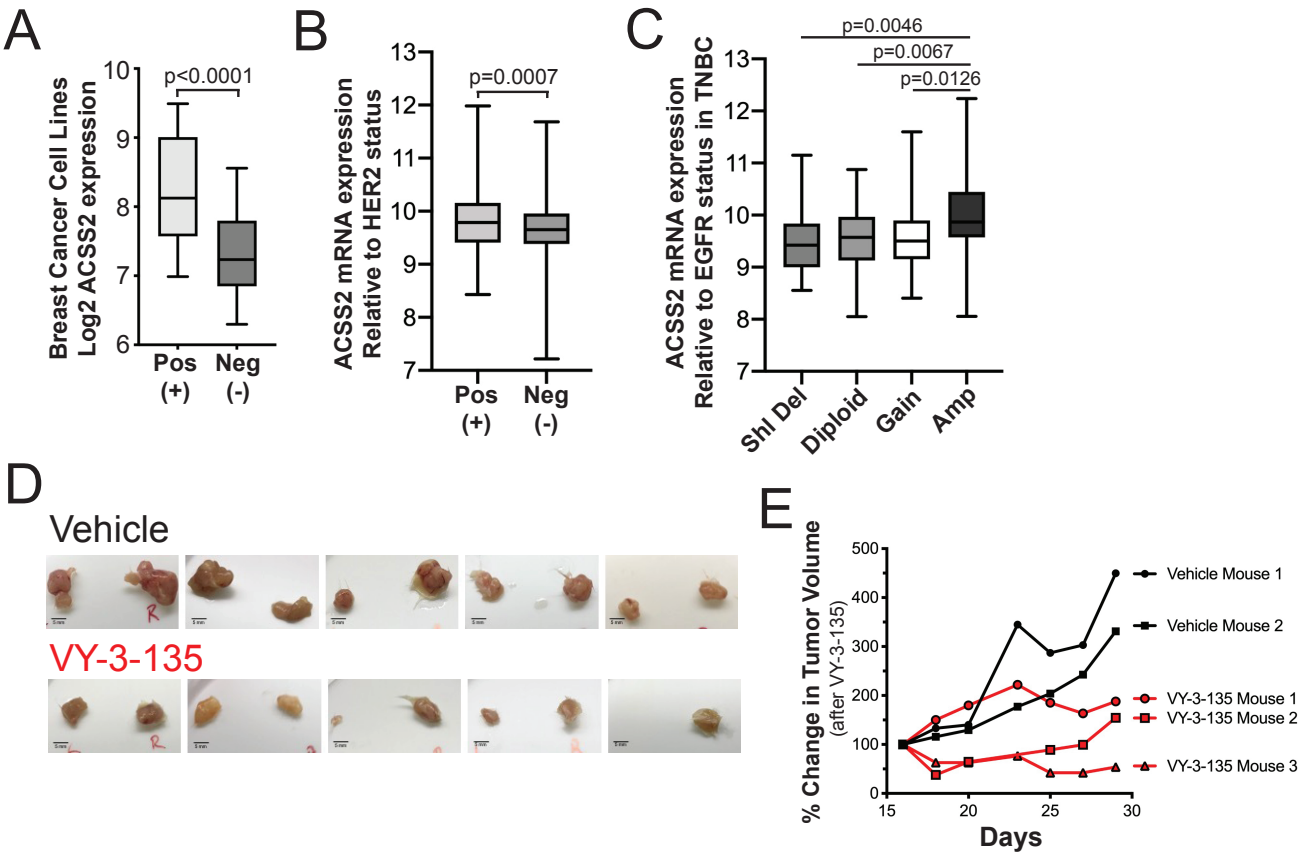

Supplementary Figure S5. VY-3-135 blocks BT474 orthograft growth. (A) Box and whiskers plot showing median, 25th to 75th percentiles, and min to max values of ACSS2 mRNA expression in human breast cancer cell lines. Pos (+) = HER2 and/or EGFR amplification. Neg (-) = no amplification. Unpaired, two tailed, Mann-Whitney test. n = 58 cell lines. (B) Box and whiskers plot showing median, 25th to 75th percentiles, and min to max values of ACSS2 mRNA expression. mRNA expression of ACSS2 in HER2+ tumors (Pos (+)) versus all other types of breast cancer (Neg (-)). Mann-Whitney test, two tailed. p value is on the graph. (C) Box and whiskers plot showing median, 25th to 75th percentiles, and min to max values of ACSS2 mRNA expression. mRNA expression of ACSS2 in TNBC patient tumors stratified by EGFR copy number alterations. Shl Del=shallow deletion, Gain=copy number gains, and Amp=gene amplification. One-way ANOVA with a Tukey's multiple comparisons test. Adjusted p values are reported on the graphs. (D) Photos show the corresponding BT474 tumors excised at the end of the study on day 28 from Fig. 5E. Scale bars = 5 mm. (E) Spider plot show percent change in tumor volume of BT474 orthograft tumors after treatment with VY-3-135.

Supplementary Figure S6

A

			BT474 tumors								
			Vehicle				VY-3-135				
FC	p	fdr	1	2	3	4	1	2	3	4	Gene Name
2.42	2E-05	13%									PDE2A
2.08	0.004	100%									MCTP2
2.07	0.004	100%									MIR210HG
2.04	0.001	100%									TNFAIP3
2.03	0.004	100%									TCN1
1.99	0.001	100%									CTD-2619J13.14
1.98	0.01	100%									HIST2H4A
1.95	0.001	100%									SNRK
1.90	0.014	100%									GJB1
1.88	0.008	100%									RP11-227G15.8
1.87	0.02	100%									SCD5
1.87	0.015	100%									TMPRSS11E
1.84	0.003	100%									CTD-2033D15.2
1.81	0.017	100%									CFD
1.79	0.007	100%									C10orf35
1.77	0.01	100%									CACNB1
1.76	0.015	100%									RNY1P9
1.73	0.031	100%									AQP1
1.72	0.022	100%									WNT2B
1.72	0.018	100%									PACSIN1
1.72	0.023	100%									SYNE3
1.70	0.028	100%									ENDOU
1.70	0.033	100%									DTX1
1.69	0.012	100%									LIN37
1.69	3E-04	100%									RAB11FIP5

B

			BT474 tumors								
			Vehicle				VY-3-135				
FC	p	fdr	1	2	3	4	1	2	3	4	Gene Name
-2.17	4E-04	100%									RP11-11N7.5
-2.06	0.004	100%									VMAC
-1.92	0.014	100%									RP11-619I22.1
-1.85	0.008	100%									RNU6-549P
-1.83	0.024	100%									ZNF337-AS1
-1.80	0.015	100%									SCML1
-1.74	0.023	100%									ENO1-IT1
-1.73	0.014	100%									ZNF93
-1.72	0.006	100%									C18orf54
-1.69	0.007	100%									TMEM220
-1.69	0.031	100%									MAP3K12
-1.68	0.037	100%									ZNF333
-1.67	0.027	100%									ACYP1
-1.67	0.02	100%									TFAP2A-AS1
-1.67	0.002	100%									RNASEH1-AS1
-1.63	0.003	100%									HSD17B7
-1.63	0.049	100%									LINC00630
-1.60	0.027	100%									RP11-319F12.2
-1.57	0.044	100%									AL133243.1
-1.57	0.018	100%									KRT17
-1.57	0.037	100%									KBTBD11
-1.56	0.005	100%									WARS2
-1.55	0.022	100%									CTB-178M22.2
-1.55	0.006	100%									ZNF678
-1.55	0.005	100%									AC007191.4

C

Type	Regulator	p	% Up	State	Z
ligand-dependent nuclear receptor	ESR1	7E-06	41	Inhibited	-2.652
chemical drug	imipramine blue	0.0003	0	Activated	2
transcription regulator	KDM5B	0.0451	0	Activated	2
chemical drug	imatinib	0.0042	33	Activated	2.425
transcription regulator	TP53	0.0064	50	Activated	3.295

D

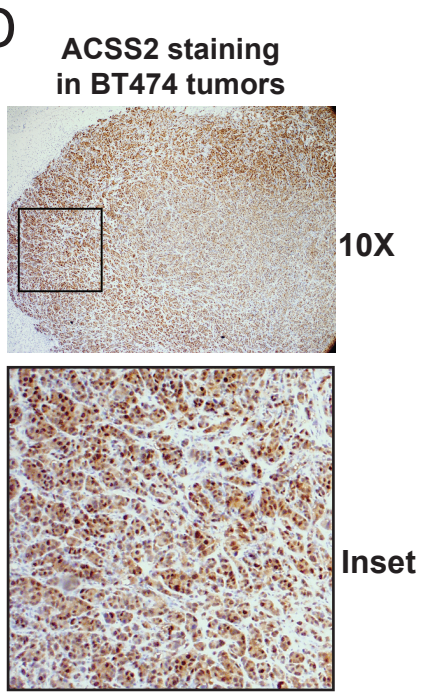

E

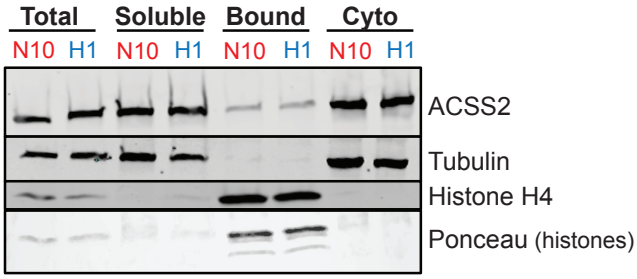

Supplementary Figure S6. ACSS2 is predominantly found in the cytosol and the soluble nuclear fraction. (A) Heatmap of QuantSeq 3´ mRNA sequencing data showing fold change, nominal p value (p), and adjusted p value (fdr). The 129 genes upregulated (nominal $p<0.05$) in BT474 tumors in response to VY-3-135 treatment. n = 4 tumors per treatment group. (B) Same as panel A showing the 119 genes downregulated (nominal $p<0.05$) in BT474 tumors in response to VY-3-135 treatment. n = 4 tumors per treatment group. (C) List of the transcriptional regulators affected by VY-3-135 as predicted by IPA. $p<0.05$ and a Z score > 2 or < -2. (D) Immunohistochemical staining of ACSS2 in a BT474 tumor. The enlarged inset shows both nuclear and cytosolic localization. (E) Nuclear fractionation of BT474 cells grown in N10 or H1 in vitro growth conditions.

Supplementary Figure S7

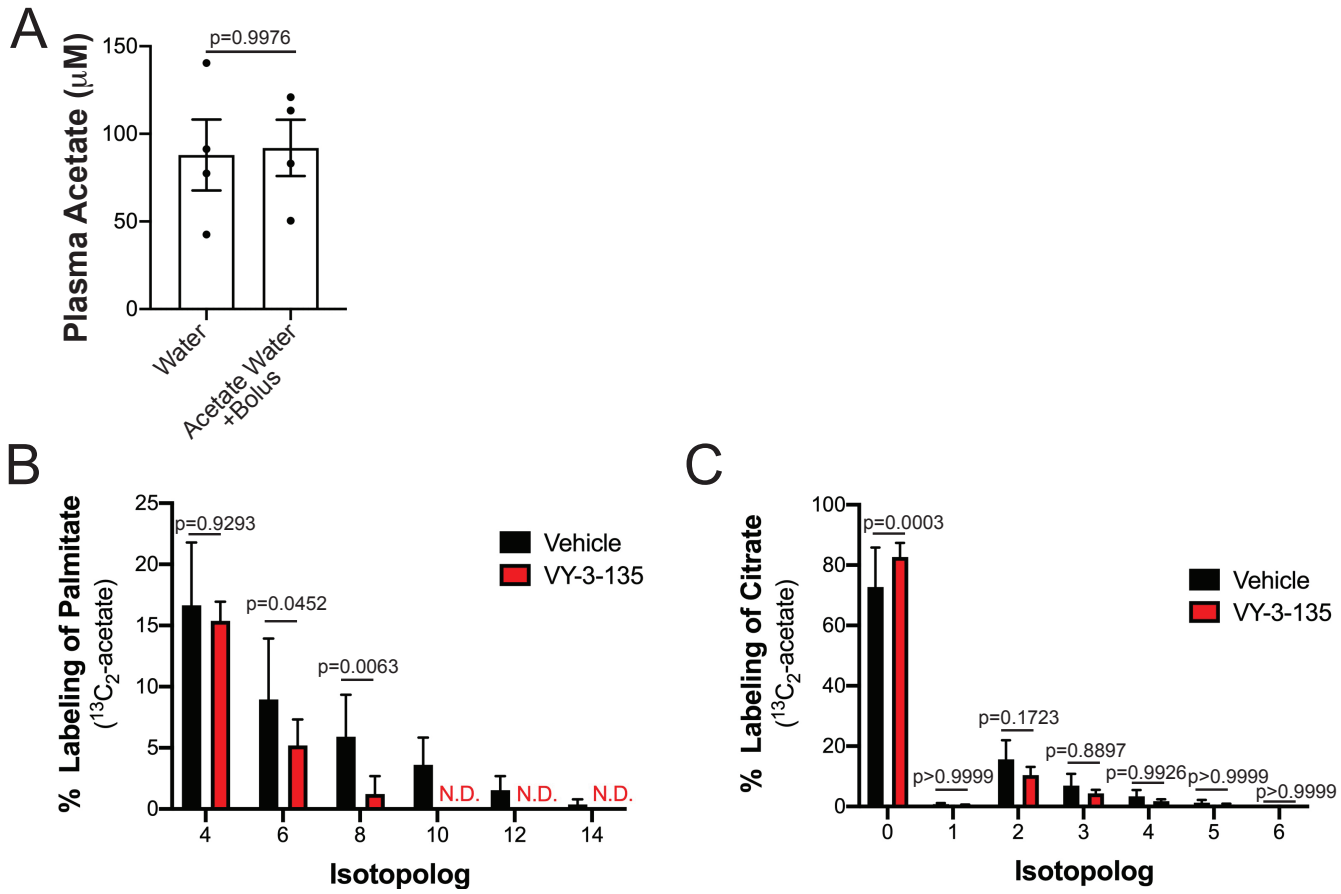

Supplementary Figure S7. VY-3-135 inhibits acetate incorporation into palmitate but not citrate. (A) Plasma acetate concentration in mice provided with 2% acetate in the drinking water for 48 hours and then a bolus of acetate (2mg/kg) 90 minutes prior to sacrifice and blood withdrawal compared to mice given only water. 2-way ANOVA p value is displayed on the graph. (B) Fractional labeling of intratumoral palmitate by $^{13}C_2$-acetate in BT474 tumors that were treated with vehicle or VY-3-135. N.D. = not detected by the mass spectrometer. Two-way ANOVA with Sidak's multiple comparisons test, adjusted p values are shown on the graph, n ≥ 6. (C) Fractional labeling of intratumoral citrate by $^{13}C_2$-acetate in BT474 tumors that were treated with vehicle or VY-3-135. Two-way ANOVA with Sidak's multiple comparisons test, adjusted p values are shown on the graph, n ≥ 6.

Supplementary Table S1

	Standard Curve						
Nominal Concentration (ng/mL)	**2**	**10**	**25**	**50**	**100**	**250**	**500**
Calculated Concentration (ng/mL)	2.02	9.56	23.9	49.4	102	261	513
n	1	1	1	1	1	1	1
Accuracy (%)	101	95.6	95.4	98.8	102	104	103

Solubility of VY-3-249:

Replicate no.	**Diluted Solution ng/mL**	**Dilution Factor**	**Solubility**
1	BLQ	10	ND*
2	BLQ		
3	BLQ		
n	3		
Mean	N/A		
SD	N/A		
CV (%)	N/A		

*ND: The solubility cannot be determined

	Standard Curve						
Nominal Concentration (ng/mL)	**2**	**10**	**25**	**50**	**100**	**250**	**500**
Calculated Concentration (ng/mL)	2.02	9.71	23.7	49.8	106	255	497
n	1	1	1	1	1	1	1
Accuracy (%)	101	97.1	95.0	100	106	102	99.4

Solubility of VY-3-135:

Replicate no.	**Diluted Solution ng/mL**	**Dilution Factor**	**Solubility µg/mL**
1	245	100	21.7
2	203		
3	202		
n	3		
Mean	217		
SD	24.8		
CV (%)	11.5		

Supplementary Table S1. VY-3-135 has better aqueous solubility than VY-3-249. Water solubility was determined against a standard curve by LC-MS/MS analysis. BLQ = below limit of quantitation. CV = coefficient of variation.